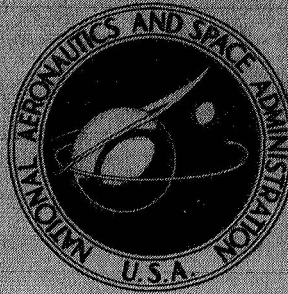


**NASA TECHNICAL  
MEMORANDUM**



**NASA TM X-1720**

**NASA TM X-1720**

**ON THE DESIGN OF ACOUSTIC LINERS  
FOR ROCKET ENGINES: MAXIMUM  
DAMPING AS A DESIGN OBJECTIVE**

*by Bert Phillips*

*Lewis Research Center  
Cleveland, Ohio*

**NATIONAL AERONAUTICS AND SPACE ADMINISTRATION • WASHINGTON, D. C. • JANUARY 1969**

NASA TM X-1720

ON THE DESIGN OF ACOUSTIC LINERS FOR ROCKET ENGINES:  
MAXIMUM DAMPING AS A DESIGN OBJECTIVE

By Bert Phillips  
Lewis Research Center  
Cleveland, Ohio

NATIONAL AERONAUTICS AND SPACE ADMINISTRATION

---

For sale by the Clearinghouse for Federal Scientific and Technical Information  
Springfield, Virginia 22151 - CFSTI price \$3.00

## ABSTRACT

A study was conducted to determine what the parameters of an acoustic liner should be to maximize liner damping. This was accomplished by solving the wave equation exactly for the frequency and damping of low order tangential and radial modes in a lined cylindrical cavity. The results, presented as dimensionless frequency and damping for each mode plotted in the impedance plane, indicate that  $\alpha$ , the acoustic absorption coefficient, can be used to design a liner provided that the liner real impedance is larger than unity.

ON THE DESIGN OF ACOUSTIC LINERS FOR ROCKET ENGINES:  
MAXIMUM DAMPING AS A DESIGN OBJECTIVE

by Bert Phillips  
Lewis Research Center

SUMMARY

A study was conducted to determine what the parameters of an acoustic liner should be to maximize liner damping. This was accomplished by solving the wave equation exactly for the frequency and damping of low order tangential and radial modes in a lined cylindrical cavity. The results, presented as dimensionless frequency and damping for each mode plotted in the impedance plane, indicate that  $\alpha$ , the acoustic absorption coefficient, can be used to design a liner provided that the liner real impedance is larger than unity.

INTRODUCTION

Extensive testing at the Lewis Research Center and elsewhere has shown that an array of Helmholtz resonators can, under certain conditions, damp combustion instability in rocket engines (refs. 1 and 2). The conditional success of some liners is indicated by the lack of correlation between high theoretical absorption coefficient,  $\alpha$ , and liner effectiveness as shown in reference 1, page 30, and reference 3. A possible reason for the disparity between theory and experiment is that, according to reference 4, the damping of acoustic waves in a cavity (combustion chamber) is maximized by maximizing  $\alpha$  only under the condition that the wave frequencies are considerably higher than the fundamental cavity or chamber resonance frequencies. The results of reference 5, however, indicate that the liner, if it is to be effective, must absorb frequencies near to the lowest resonant frequencies of the chamber. Consequently, it is not clear that maximizing the acoustic absorption coefficient,  $\alpha$ , is the proper design objective.

To determine what the parameters of an acoustic liner should be to maximize the damping of a liner, the exact solutions for the tangential and radial acoustic modes in a closed end (no flow) cylindrical cavity with absorbing walls were obtained. The approach

is similar to that presented in reference 6 without the combustion driving and nozzle damping. The study presented in reference 6, however, made no attempt to investigate what parameter of a liner would maximize the liner damping. To facilitate the use of the results by engine designers, the results are presented as the normalized frequency and damping for each mode as functions of the liner parameter  $\bar{\theta}$ , the real part of the acoustic impedance (resistance) and  $\bar{X}$ , the imaginary part of the acoustic impedance (reactance). The solutions were obtained by the use of a program for calculating complex Bessel functions reported in reference 7. Since combustion instability only involves the lower order resonant modes, only the lower order solutions will be presented.

## THEORY

The equation for acoustic waves in a cylindrical cavity with closed ends, no mean flow, and uniform gas properties is:

$$\frac{\partial^2 p}{\partial r^2} + \frac{1}{r} \frac{\partial p}{\partial r} + \frac{1}{r^2} \frac{\partial^2 p}{\partial \varphi^2} + \frac{\partial^2 p}{\partial z^2} = \frac{1}{c^2} \frac{\partial^2 p}{\partial t^2} \quad (1)$$

where

$p$  oscillatory pressure, lbf/ft<sup>2</sup>

$r$  radial distance, ft

$z$  axial distance, ft

$\varphi$  azimuthal angle, rad

$c$  cavity sonic velocity, ft/sec

$t$  time, sec

For a transverse mode with no axial dependence and exponential time variation, a solution for equation (1) is:

$$p = PJ_n \left[ \frac{\pi r}{a_0} (\mu_n + ik_n) \right] \cos n\varphi \exp(i\omega t - kt) \quad (2)$$

$J_n$  Bessel function of first kind of order  $n$ ,  $n = 0, 1, \dots$

$a_0$  cavity radius, ft

$\omega$  angular frequency, rad/sec

- k            temporal damping constant, 1/sec  
 $\mu_n, k_n$     distribution coefficients resulting from cavity walls that are not infinitely hard  
P            maximum value of oscillatory pressure, lbf/ft<sup>2</sup>

Substituting equation (2) into equation (1):

$$-\left(\frac{a_0}{c}\right)^2 (\omega - k)^2 = [\pi(\mu_n + ik_n)]^2 \quad (3)$$

This expression gives the relation between the oscillation frequency, the decay constant, and the distribution coefficients. The next step is to solve for the distribution coefficients in terms of the wall resistance and reactance,  $\bar{\theta}$  and  $\bar{X}$ .

The radial acoustic particle velocity into the wall is:

$$u_r = \frac{i}{\frac{\omega\rho}{g_c}} \frac{\partial\rho}{\partial r} \Big|_{r=a_0} \quad (4)$$

- $u_r$     radial velocity, ft/sec  
 $\rho$     gas density, lbm/ft<sup>3</sup>  
 $g_c$     gravitational constant, (lbm/lbf)(ft/sec<sup>2</sup>)

Substituting equation (2) into equation (4) and setting  $n = 1$  (first tangential mode)

$$u_r = \frac{iP}{\omega\rho a_0} \cos\theta \exp(i\omega t - kt) \left\{ \pi(\mu_n + ik_n) J_0 \left[ \frac{\pi r}{a_0} (\mu_n + ik_n) \right] - J_1 \left[ \frac{\pi r}{a_0} (\mu_n + ik_n) \right] \right\} \quad (5)$$

For clarity, the quantity  $(\mu_n + ik_n)$  is redefined, as in reference 7, as  $R e^{ih}$ , where  $R$  is the distribution coefficient magnitude and  $h$  the distribution coefficient angle.

$$\pi(\mu_n + ik_n) = R \cos(h) + i R \sin(h) \quad (6)$$

Dividing equation (5) into equation (2) and defining  $\eta = \omega a_0 / \pi c$  the following equation results:

$$\frac{P}{\frac{\rho}{g_c} c u_r \eta} = \frac{i\pi}{\operatorname{Re}^{ih} \frac{J_0(\operatorname{Re}^{ih})}{J_1(\operatorname{Re}^{ih})} - 1} \quad (7)$$

The quantity  $P/[(\rho/g_c)u_r c]$  is the impedance which can also be expressed as the sum of a real and imaginary part,

$$\frac{P}{\frac{\rho}{g_c} u_r c \eta} = \frac{\bar{\theta}}{\eta} + i \frac{\bar{X}}{\eta} \quad (8)$$

where

$\eta$  wavelength ratio defined by  $\omega a_0 / \pi c = D/\lambda$

$D$  cavity diameter

$\lambda$  wavelength

$\bar{\theta}, \bar{X}$  normalized resistance and reactance

By choosing values of  $R$  and  $h$ , equations (7) and (8) can be solved for  $\bar{\theta}/\eta$  and  $\bar{X}/\eta$ .

Combining equations (3) and (6), it can be shown that

$$\frac{ka_0}{c} = R \sin(h) \quad (9)$$

$$\frac{\omega a_0}{c} = R \cos(h) \quad (10)$$

These are the normalized damping rates and resonant oscillation frequencies of the cavity for the given values of  $R$  and  $h$ . Therefore, by specifying  $R$  and  $h$ ,  $\omega a_0/c$ , and  $\eta$  can be calculated and, from equation (8),  $\bar{\theta}$  and  $\bar{X}$  can be determined.

## RESULTS AND DISCUSSION

### Defining Modes of Oscillation

Modes of acoustic wave oscillation in cavities are generally defined by the values of

$\omega a_0/c$  that satisfy the condition that  $u_r$ , the radial velocity at the wall, is zero. For the case of nonzero admittance, and, in particular, for  $\bar{\theta} \cong 1$ , mode definition becomes quite difficult. The approach taken in the present report was to define the modes based on the value of  $R$ , defined by equation (6). This approach has some justification since, in the limit of hard walls ( $h = 0^\circ$ ,  $\bar{\theta} = \infty$ ),  $R = \omega a_0/c$  and each mode has a single value of  $R$ . To determine the behavior of  $R$  in the region of interest ("soft walls"), lines of constant  $R$  were plotted in the  $\bar{\theta} - \bar{X}$  plane, as shown in figure 1. The  $J_0$  Bessel function was chosen for illustration. For all of the  $R$  values shown in the figure,  $R$  at  $h = 0^\circ$  is on the abscissa ( $\bar{\theta} = 0$ ); as  $h$  is increased, the line spirals in toward the origin until, at  $h = 90^\circ$ , all values of  $R$  intersect the origin. For  $R = 0.5$ , the  $h = 0^\circ$  point is at  $\bar{X} = 3.074$ ,  $\bar{\theta} = 0^\circ$ . As  $R$  is increased, the  $h = 0^\circ$  point on the abscissa moves left toward the origin until, at  $R \cong 2.42$ , the line intersects itself at  $h = 0^\circ$  and  $90^\circ$ . Between  $R = 2.42$  and  $3.05$ , the lines of constant  $R$  cross. An example is  $R = 2.80$  which crosses at point A on figure 1, corresponding to  $h = 3^\circ$  and  $66^\circ$ . Continuing to increase  $R$  beyond  $3.05$  moves the  $h = 0^\circ$  point to the left until, at  $R$  very close to  $3.83$ , the  $h = 0^\circ$  point is at  $\bar{X} = -\infty$ . At  $R$  exactly equal to  $3.83$ , the  $h = 0^\circ$  point is at  $\bar{\theta} = \infty$ ,  $\bar{X} = 0$ . For  $R > 3.83$ , the  $h = 0^\circ$  point swings to  $\bar{X} = +\infty$  and again moves to the left with increasing values at  $R$ . The process continues as  $R$  increases, with lines of constant  $R$  crossing within certain ranges.

The same results are obtained with  $J_1, J_2$ , etc., giving rise to a series of curves in

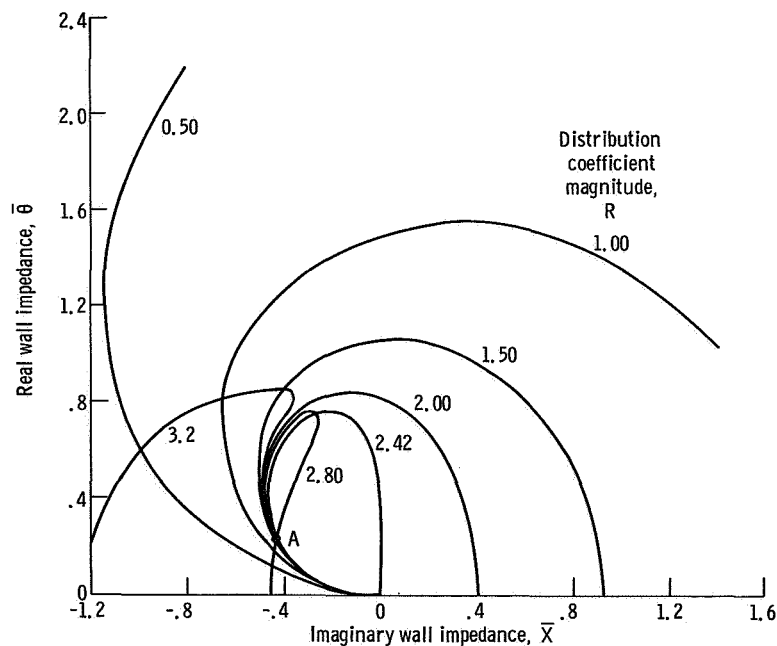


Figure 1. - Lines of constant distribution coefficient magnitude as function of real and imaginary wall impedance.

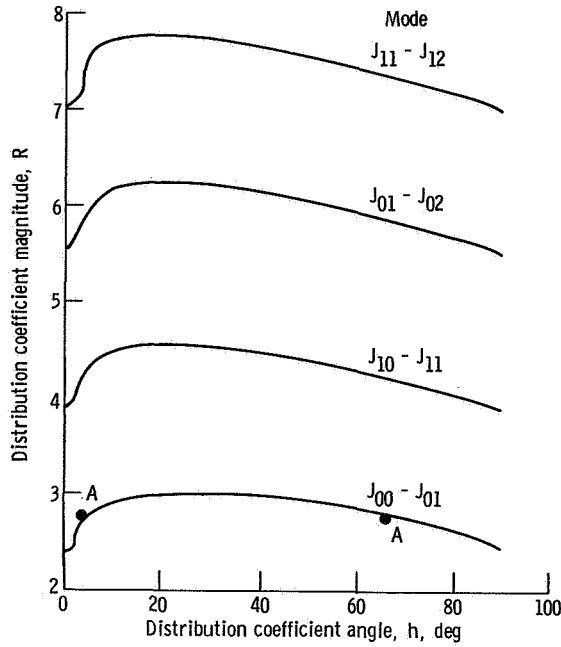


Figure 2. - Values of distribution coefficient magnitude and angle designating mode boundaries.

the  $R, h$  plane defined by the values of  $R$  and  $h$  at the crossings. Four of these curves are shown in figure 2. On the  $J_{00} - J_{01}$  curve, the two points, labeled A, correspond to point A on figure 1. These curves in the  $R - h$  plane are arbitrarily taken as the boundaries of modes. All values of  $R$  and  $h$  below the  $J_{00} - J_{01}$  curve are in the  $J_{00}$  mode, all values of  $R$  and  $h$  between the  $J_{10} - J_{11}$  and the  $J_{11} - J_{12}$  curves are in the  $J_{11}$  mode, etc. Thus by defining the value of  $R$  and  $h$ , we can confine our discussion to a particular mode.

### Modal Resonant Frequencies and Damping

Using the previously obtained  $R-h$  criterion, the fundamental dimensionless resonance frequencies and damping of each mode can be calculated as functions of  $\bar{\theta}$  and  $\bar{X}$ . These results are displayed as lines of constant  $\omega a_0/c$  and  $ka_0/c$  in the  $\bar{\theta}, \bar{X}$  plane. The results for the  $J_{00}$  mode are presented in figures 3(a) and (b). The  $J_{00}$  mode is presented first although it has no real physical significance since the fundamental resonance frequency of a  $J_{00}$  mode for hard walls is 0.

The lines of constant  $\omega a_0/c$  in figure 3(a) resemble those of constant  $R$ . In the region  $\left\{ \begin{array}{l} 0.8 > \bar{\theta} > 0 \\ 0 > \bar{X} > -0.6 \end{array} \right\}$ , all the lines of constant frequency converge, resulting in a zone

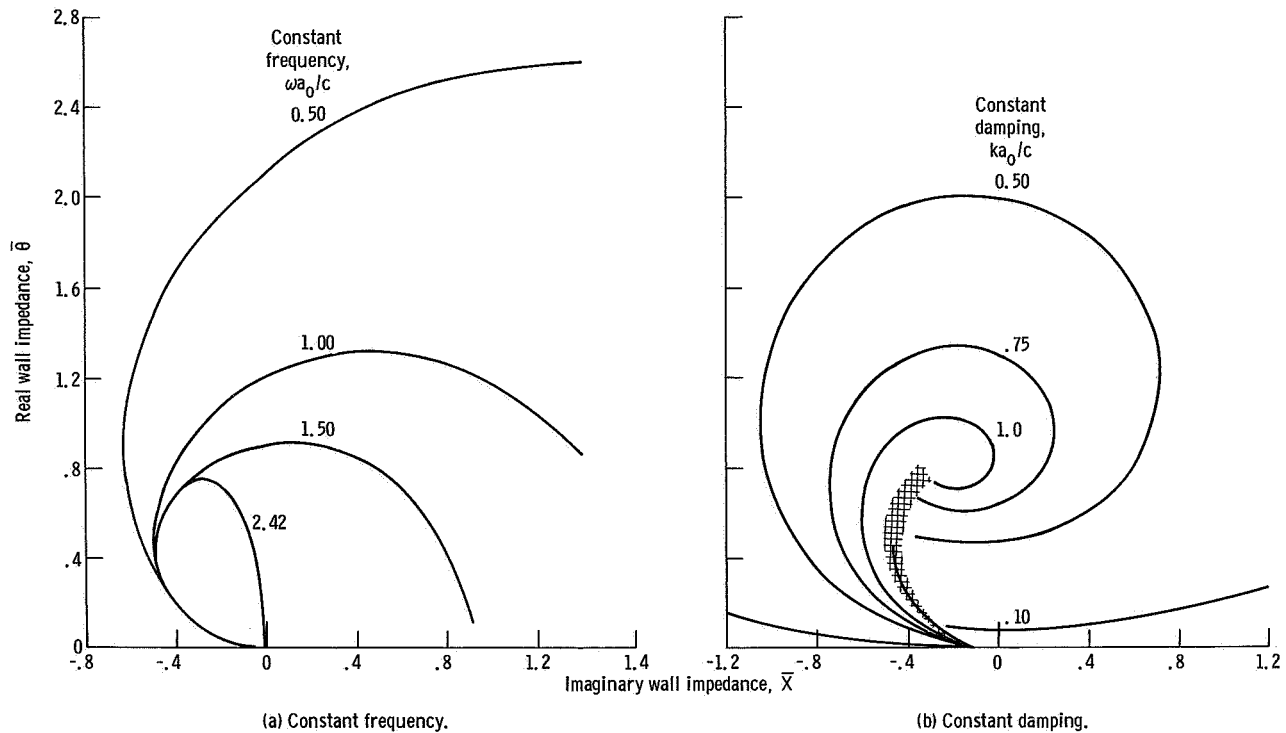


Figure 3. - Lines of constant frequency and constant damping as function of real and imaginary wall impedance for  $J_{00}$  mode.

where the resonant frequency is not well defined, that is, small changes in either  $\bar{\theta}$  or  $\bar{X}$  can result in large changes in  $\omega a_0/c$ . As  $\omega a_0/c$  is increased to 2.42 and greater, the lines of constant frequency intersect in the same manner as lines of constant  $R$  in figure 1. The interpretation can be made that, in this region, both the  $J_{00}$  and the  $J_{01}$  mode have the same resonant frequencies. The results indicate that the resonant frequency for the mode can be specified readily anywhere in the  $\bar{\theta} - \bar{X}$  plane except for the region already mentioned ( $\theta \leq 0.8$ ).

The behavior of the damping for the  $J_{00}$  mode was determined in the same manner as the frequency and is shown in figure 3(b). The lines of constant damping begin at the origin and spiral clockwise until the corresponding values of  $R$  and  $h$  on the lines of constant  $ka_0/c$  correspond to the upper bound of the mode, where the line is terminated. The region of maximum damping, indicated by the cross-hatching, on the figure corresponds to the upper bound of the mode, and, in addition, corresponds to the region of ill-defined frequency of figure 3(a). Thus, both frequency and damping for the mode can be specified except for the same cross hatched regions. Although the discussion of the damping characteristics of the  $J_{00}$  mode is, by no means, completed, it may be more instructive to go on to the next solution of  $J_0$ , the  $J_{01}$  mode.

The lines of constant frequency and damping are presented on figures 4(a) and (b). The results on figure 4(a) are similar to those presented in figure 3(a), however, the

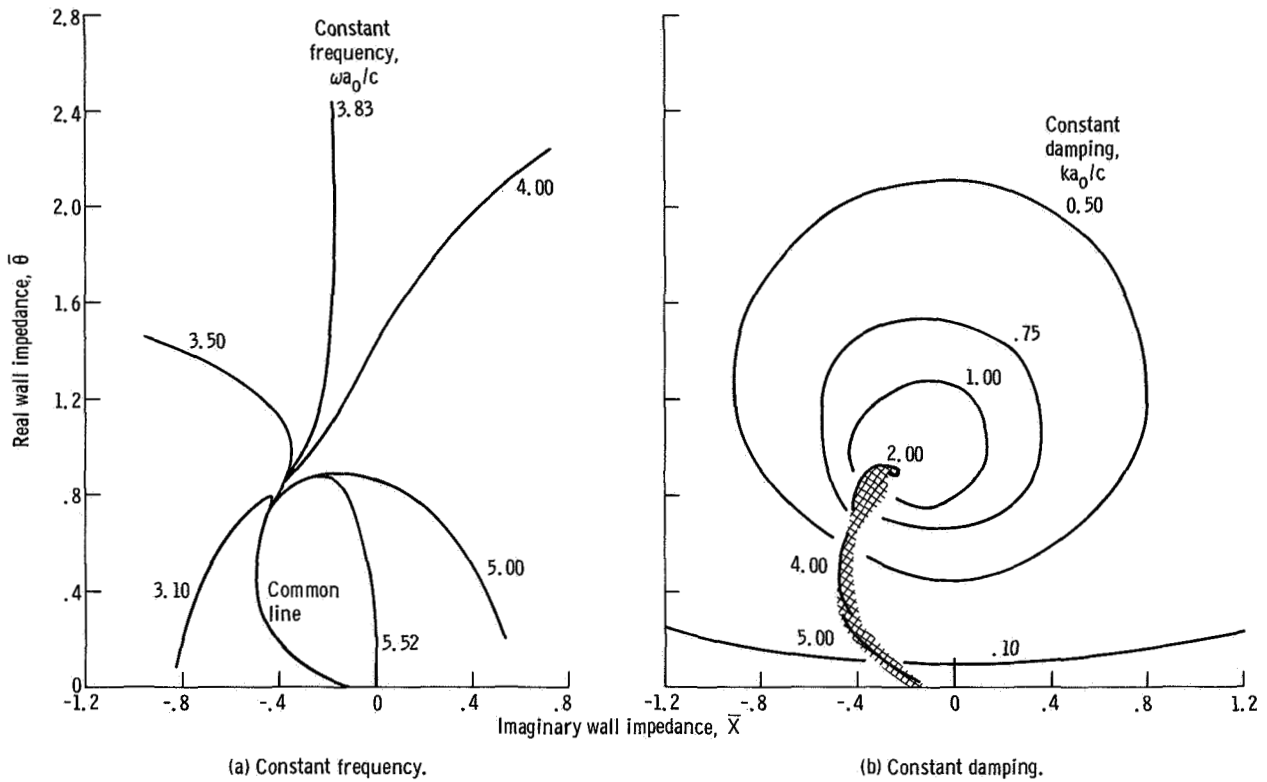


Figure 4. - Lines of constant frequency and constant damping as function of real and imaginary wall impedance for  $J_{01}$  mode.

resonant frequency of the  $J_{01}$  mode in the limit of hard walls is not zero. The line representing  $\omega a_0/c = 3.83$  continues upwards, representing the resonant frequency of the  $J_{01}$  or first radial mode for hard walls. In the limit of large  $\bar{\theta}$ , as the reactance,  $\bar{X}$ , becomes negative, the line of constant frequency for values less than 3.83 fall to the left, that is, the resonant frequency decreases. If there is a positive wall impedance,  $\bar{X} > 0$ , the  $J_{01}$  resonant frequency becomes greater than 3.83. This result confirms the experimental and theoretical approximation results of reference 9. In the same manner as figure 3(a), there is a region of poor definition in the frequency where the lines of constant  $\omega a_0/c$  converge.

The lines of constant damping for the  $J_{01}$  mode are presented in figure 4(b). The results are quite different from those of figure 3(b) and show lines of damping that are approximately closed concentric curves except for the cross-hatched area. If the high damping in the cross-hatched area can, for the moment, be disregarded, the results may be interpreted as defining zones of maximum damping in the region of  $\bar{\theta} = 1$ ,  $\bar{X} = 0$ . For comparison, lines of constant  $\alpha$ , the absorption coefficient, are plotted in the impedance plane and are shown in figure 5. The absorption coefficient,  $\alpha$ , which maximizes in the same region,  $\bar{\theta} = 1$ ,  $\bar{X} = 0$ , is an appropriate design criterion, since maximizing  $\alpha$  would maximize the true damping.

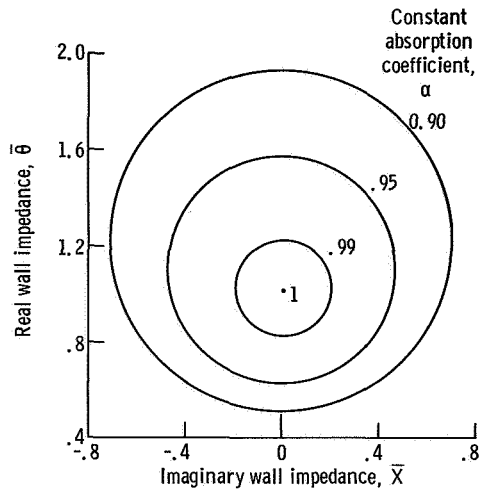


Figure 5. - Lines of constant absorption coefficient as function of real and imaginary wall impedance.

It is important, however, to investigate any advantage in designing a liner for the region of maximum damping indicated by the cross-hatched area. Consider the  $J_{01}$  mode for  $\bar{\theta}$  less than unity with  $\bar{X} = -2$ ; if the liner tuning could be gradually improved so as to make  $\bar{X}$  less negative, the resonant frequency would gradually decrease as per figure 4(a) until the common line representing all the frequencies was reached.

As  $\bar{X}$  approaches  $-0.4$  from the left, the damping, according to 4(b), sharply increases at the cross-hatched region. The frequency, however, as per figure 4(a), is near the common line and the system is now operating in the regime where both the  $J_{00}$  and  $J_{01}$  modes have the same frequency. Any system, given a situation where it can resonate at the same frequency with two widely different damping rates will appear to decay at the lower damping rate since the higher damping wave will not be evident. In the case under discussion, the system will decay at the lower damping rate corresponding to the  $J_{00}$  mode. In addition, the oscillatory pressure profile will generally shift to that corresponding to the mode that has the lower damping. Consequently, it does not appear that any advantage could be gained by designing for the cross-hatched region of damping. If, therefore, the cross-hatched region were disregarded in designing a liner,  $\alpha$  could properly be used for the first radial mode, provided that the values of  $\bar{\theta}$  were maintained above unity, and away from the cross-hatched region.

The next system to be investigated was the  $J_{10}$  or first tangential mode. A plot of the lines of constant frequency in the  $\bar{\theta} - \bar{X}$  plane is shown in figure 6(a). The results appear to be similar to those presented in figure 4(a). In this case, however, the resonant frequency corresponding to the first tangential mode with "hard walls" ( $\theta \approx \infty$ ), is 1.84. In addition, the effects of positive and negative impedance on the resonant frequency in the region of large  $\bar{\theta}$  are consistent with those of figure 4(a). The region cor-

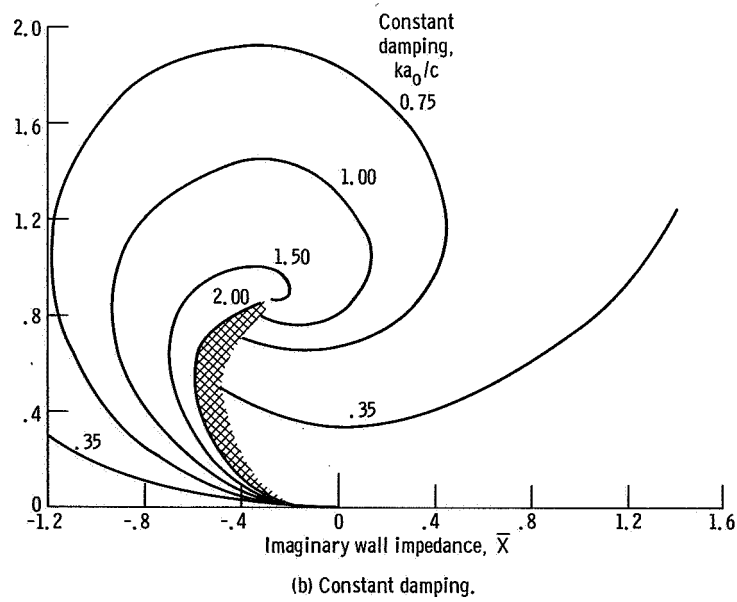
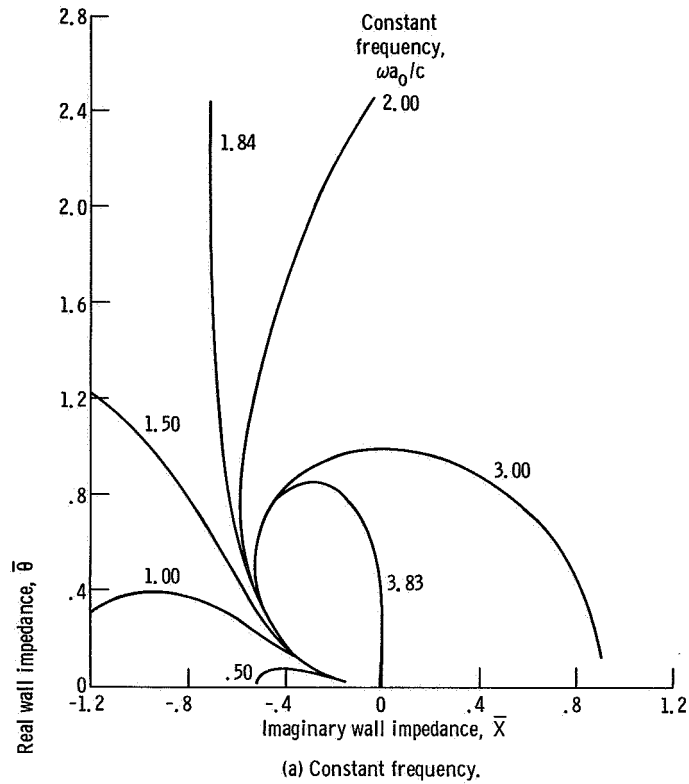


Figure 6. - Lines of constant frequency and constant damping as function of real and imaginary wall impedance for  $J_{10}$  mode.

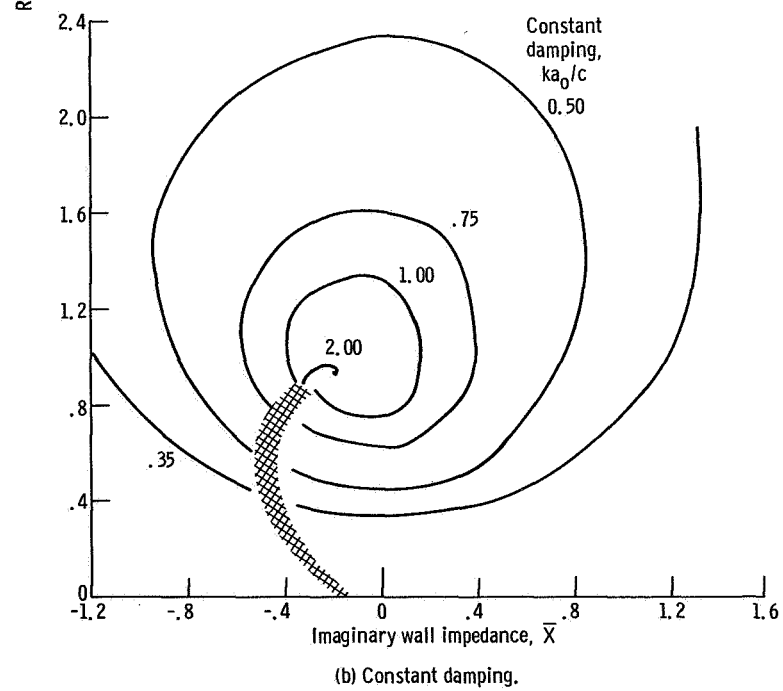
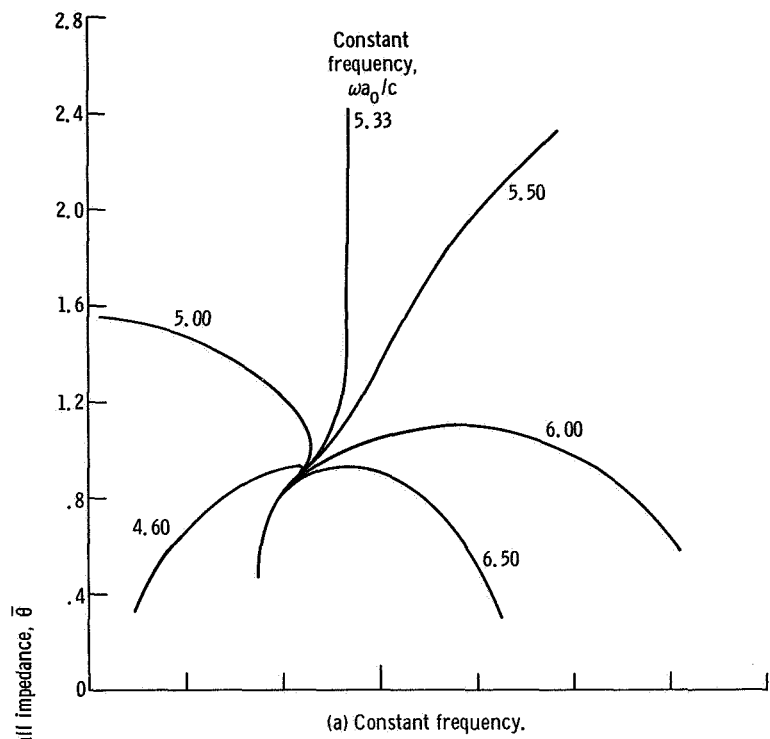


Figure 7. - Lines of constant frequency and constant damping as function of real and imaginary wall impedance for  $J_{11}$  mode.

responding to ill-defined resonant frequency is an area in the same position as that region for the  $J_0$  modes.

The lines of constant damping for the  $J_{10}$  mode are shown on figure 6(b). The results resemble those for the  $J_{00}$  mode as shown in figure 3(b) with the region of maximum damping in the same position. Following the same approach as with the  $J_0$  modes, the discussion of the  $J_{11}$  mode is now in order. The frequency and damping results for the  $J_{11}$  mode are presented in figures 7(a) and (b). The frequency in the limit of  $\bar{\theta} = \infty$  for this mode is 5.33 corresponding to the first tangential-first radial mode with "hard walls." The damping for the  $J_{11}$  mode is, with the exception of the cross-hatched area, a set of closed curves of lines of constant damping with the maximum values in the  $\bar{\theta} \sim 1$ ,  $\bar{X} \sim 0$  area.

Continuing both the  $J_0$  and  $J_1$  solutions, a set of figures for both the frequency and damping can be obtained. In all of the cases, the lines of constant damping will be closed curves with the exception of the cross-hatched region which is common to all the modes. This cross-hatched region can be regarded as the operating point at which modes can readily be altered at constant frequency. Given a system with a driver with finite bandwidth, operation anywhere in the region  $\bar{\theta} < 1$ ,  $\bar{X} < 0$  will encourage the system to switch to the lower damping mode.

## CONCLUDING REMARKS

The conclusion that one can come to with regard to the results presented is that  $\alpha$  can be used to design a liner which will damp low order transverse cylindrical modes provided that the real impedance is maintained at values greater than unity. Operating at a value less than unity with negative imaginary impedance may result in the damping of one mode and the appearance of another.

Lewis Research Center,  
National Aeronautics and Space Administration,  
Cleveland, Ohio, October 9, 1968,  
128-31-06-05-22.

## REFERENCES

1. Wanhainen, John P.; Bloomer, Harry E.; Vincent, David W.; and Curley, Jerome K.: Experimental Investigation of Acoustic Liners to Suppress Screech in Hydrogen-Oxygen Rockets. NASA TN D-3822, 1967.

2. Anon. : A Study of the Suppression of Combustion Oscillations with Mechanical Damping Devices, Phase II - Summary Report. Rep. PWA-FR-1922, Pratt & Whitney Aircraft, July 5, 1966.
3. Anon. : F-1 Engine Acoustic Absorber Task. Rep. R-7011, Rocketdyne Div., North American Aviation, Inc. (NASA CR-89431), July 31, 1967.
4. Morse, Philip M. : Vibration and Sound. Second Ed., McGraw-Hill Book Co., Inc., 1948.
5. Phillips, Bert: Experimental Investigation of an Acoustic Liner with Variable Cavity Depth. NASA TN D-4492, 1968.
6. Priem, Richard J.; and Rice, Edward J. : Combustion Instability with Finite Mach Number Flow and Acoustic Liners. Paper presented at the 12th International Symposium on Combustion Poitiers, France, July 14-20, 1968.
7. Rice, Edward J. : Attenuation of Sound in Soft Walled Circular Ducts. Paper Presented at Symposium on Aerodynamic Noise, AFOSR, Institute for Aerospace Research, Univ. of Toronto, May 20-21, 1968.
8. Molloy, Charles T.; Honigman, Esther: Attenuation of Sound in Lined Circular Ducts. J. Acoust. Soc. Am., vol. 16, no. 4, Apr. 1945, pp. 267-272.
9. Phillips, Bert; and Morgan, C. Joe: Mechanical Absorption of Acoustic Oscillations in Simulated Rocket Combustion Chambers. NASA TN D-3792, 1966.

POSTMASTER: If Undeliverable (Section 158,  
Postal Manual) Do Not Return

*"The aeronautical and space activities of the United States shall be conducted so as to contribute . . . to the expansion of human knowledge of phenomena in the atmosphere and space. The Administration shall provide for the widest practicable and appropriate dissemination of information concerning its activities and the results thereof."*

— NATIONAL AERONAUTICS AND SPACE ACT OF 1958

## NASA SCIENTIFIC AND TECHNICAL PUBLICATIONS

**TECHNICAL REPORTS:** Scientific and technical information considered important, complete, and a lasting contribution to existing knowledge.

**TECHNICAL NOTES:** Information less broad in scope but nevertheless of importance as a contribution to existing knowledge.

**TECHNICAL MEMORANDUMS:** Information receiving limited distribution because of preliminary data, security classification, or other reasons.

**CONTRACTOR REPORTS:** Scientific and technical information generated under a NASA contract or grant and considered an important contribution to existing knowledge.

**TECHNICAL TRANSLATIONS:** Information published in a foreign language considered to merit NASA distribution in English.

**SPECIAL PUBLICATIONS:** Information derived from or of value to NASA activities. Publications include conference proceedings, monographs, data compilations, handbooks, sourcebooks, and special bibliographies.

**TECHNOLOGY UTILIZATION PUBLICATIONS:** Information on technology used by NASA that may be of particular interest in commercial and other non-aerospace applications. Publications include Tech Briefs, Technology Utilization Reports and Notes, and Technology Surveys.

*Details on the availability of these publications may be obtained from:*

**SCIENTIFIC AND TECHNICAL INFORMATION DIVISION  
NATIONAL AERONAUTICS AND SPACE ADMINISTRATION  
Washington, D.C. 20546**